

# Phase correction and resolution improvement of digital holographic image in numerical reconstruction with angular multiplexing

Xiaobo Yan (闫晓博), Jianlin Zhao (赵建林)\*, Jianglei Di (邸江磊), Hongzhen Jiang (姜宏振),  
and Weiwei Sun (孙伟伟)

Institute of Optical Information Science and Technology, Shaanxi Key Laboratory of Optical Information Technology,  
School of Science, Northwestern Polytechnical University, Xi'an 710072, China

\*E-mail: jlzhao@nwpu.edu.cn

Received July 16, 2009

A phase correction method is presented to remove the phase slope of the sub-holograms caused by the multi-direction illumination on object in digital holography. To improve the resolution of the reconstructed holographic images, two sub-holograms are recorded by using angular multiplexing and their phase slope parameter is obtained by theoretical analysis. Introducing a phase correction parameter to this phase slope, the ideal complex reconstructed image can be obtained by superposing the reconstructed object wave fields of the two sub-holograms. Experimental results demonstrate that the resolution of the reconstructed image can be effectively enhanced.

OCIS codes: 090.1995, 100.2000, 100.3010.

doi: 10.3788/COL20090712.1072.

In recent years, with the development of the computer and digital image processing technology, digital holography (DH)<sup>[1-3]</sup> has been widely applied in many fields such as microscopy<sup>[4-7]</sup>, characterization of micro-electro-mechanical systems (MEMS)<sup>[8]</sup>, color display<sup>[9]</sup>, information encryption<sup>[10]</sup>, vibration measurement<sup>[11]</sup>, and so on. However, because of the limited target size and low spatial resolution of the charge-coupled device (CCD) used to record the digital holograms, it is difficult to directly obtain a holographic image with high resolution. To solve this problem, the synthetic aperture digital holography<sup>[12,13]</sup> was proposed to compose a larger hologram from several sub-holograms recorded in different positions by the same CCD. However, this approach was time consuming and had vast data processing. Recently, Yuan *et al.* recorded multiple sub-holograms with angular multiplexing in pulsed digital holography<sup>[14]</sup>, but the time delay between three pulse pairs needed to be accurately adjusted to ensure incoherent overlapping of sub-holograms. Mico *et al.* proposed an aperture synthesis approach with a (VCSEL) array<sup>[15]</sup>, but a specially designed mask was needed to avoid incorrect spectrum overlapping. Liu *et al.* presented a method for collecting high frequency components of the object wavefront with an appropriate diffractive optical element inserted in the optical path<sup>[16]</sup>, which was limited for improvement of the resolution of the reconstructed image.

A series of sub-holograms can be recorded in one composite CCD frame with angular multiplexing in DH. Each of them covers different regions of the spatial spectrum for the multi-direction illumination on object, and can be independently reconstructed after the digital spatial filtering in the Fourier spectral domain. This is equivalent to enlarge the numerical aperture (NA) of the holographic recording system and improve the resolution of the synthesized reconstructed image, but there would be a phase slope parameter between the reconstructed object wavefronts of different sub-holograms, which will af-

fect the quality of the complex reconstructed image. In this letter, we propose and demonstrate a phase correction method for eliminating the phase slope.

The recording method of the hologram is displayed in Fig. 1, where  $(x_o, y_o)$  and  $(x_h, y_h)$  denote the coordinates of the object and the hologram plane, respectively. The object is illuminated by two plane waves  $O_1$  and  $O_2$  with different incident angles.  $O_1$  and  $O_2$  are firstly modulated by the object transmission function  $t(x_o, y_o)$ , and then arrive at the recording plane of the hologram via the Fresnel diffraction, marked as  $D_1$  and  $D_2$ , respectively.  $D_1$  and  $D_2$  can be written as

$$D_n = \frac{\exp(ikd)}{i\lambda d} \exp\left[\frac{ik}{2d}(x_h^2 + y_h^2)\right] \\ \times \iint O_n t(x_o, y_o) \exp\left[\frac{ik}{2d}(x_o^2 + y_o^2)\right] \\ \times \exp\left[-\frac{ik}{d}(x_o x_h + y_o y_h)\right] dx_o dy_o, \quad (n = 1, 2) \quad (1)$$

where  $d$  is the recording distance,  $k = 2\pi/\lambda$ , and  $\lambda$  is the wavelength. A reference wave  $R$  interferes with  $D_1$  and  $D_2$  in the recording plane, respectively, and the intensity distribution of the recorded hologram  $I_h$  can be expressed as

$$I_h = |R + D_1|^2 + |R + D_2|^2 = 2|R|^2 + |D_1|^2 \\ + |D_2|^2 + RD_1^* + R^*D_1 + RD_2^* + R^*D_2, \quad (2)$$

where the two interfering terms  $R^*D_1$  and  $R^*D_2$  correspond to the original wave field of the object. In the Fourier transform domain of the hologram, the spatial spectrum of the two interfering terms  $R^*D_1$  and  $R^*D_2$  can be separated via the spectrum filtering, respectively. Then two diffraction fields  $D_1$  and  $D_2$  are obtained by inverse Fourier transform for the separated spectrum, respectively, and the reconstructed original object wave-

front in the object plane can be obtained by

$$\begin{aligned} \Psi_n &= \frac{\exp(ikd')}{i\lambda d'} \exp\left[\frac{ik}{2d'}(x_o^2 + y_o^2)\right] \times \\ &\iint RR^* D_n \exp\left[\frac{ik}{2d'}(x_h^2 + y_h^2)\right] \times \\ &\exp\left[-\frac{ik}{d'}(x_o x_h + y_o y_h)\right] dx_h dy_h \\ &= CO_n t(x_o, y_o), \quad (n = 1, 2) \end{aligned} \quad (3)$$

where  $\Psi_n$  is the reconstructed wavefront in the object plane,  $C$  is a constant,  $d' = -d$  is the reconstructed distance.

In the recording process, there exists an angle between two wavefronts of the object waves, so that a corresponding phase slope parameter exists between the two reconstructed phase planes of the object wavefronts. Supposing that  $O_1 = A$ , and  $O_2 = A \exp[ik(x_o \cos\alpha + y_o \cos\beta)]$ , we can obtain  $\Psi_1$  and  $\Psi_2$  from Eq. (3) as

$$\begin{cases} \Psi_1 = CA t(x_o, y_o) \\ \Psi_2 = CA t(x_o, y_o) \times \exp[ik(x_o \cos\alpha + y_o \cos\beta)] \end{cases}, \quad (4)$$

where  $\alpha$  and  $\beta$  are the angles of  $O_2$  to  $x$  and  $y$  axes, respectively, and  $A$  is the amplitude. Comparing  $\Psi_1$  with  $\Psi_2$ , it is found that there is a linear phase parameter  $\exp[ik(x_o \cos\alpha + y_o \cos\beta)]$  between  $\Psi_1$  and  $\Psi_2$ . If  $\Psi_1$  and  $\Psi_2$  are superposed directly, the intensity distribution of the synthetic complex amplitudes will be expressed as

$$\begin{aligned} |\Psi_1 + \Psi_2|^2 &= |\Psi_1|^2 + |\Psi_2|^2 + \Psi_1 \Psi_2^* + \Psi_1^* \Psi_2 \\ &= 2|CA t(x_o, y_o)|^2 + 2|CA t(x_o, y_o)|^2 \\ &\quad \times \cos[k(x_o \cos\alpha + y_o \cos\beta)]. \end{aligned} \quad (5)$$

It is noticed that the complex reconstructed image of the two sub-holograms will produce interference from Eq. (5). To resolve this problem, we introduce a phase correction parameter  $\varphi = \exp[-ik(x_o \cos\alpha + y_o \cos\beta)]$ . Multiplying  $\Psi_2$  with  $\varphi$ , the phase slope can be corrected ideally. The complex wave field reconstructed by the two sub-holograms is obtained finally by

$$\Psi = \Psi_1 + \varphi \Psi_2. \quad (6)$$

Figure 2 shows the experimental setup which is analogous to a Mach-Zehnder interferometer. A laser with a power of 60 mW and a wavelength of 532 nm is used as the light source. The recorded object is a resolution test target with the size of  $0.4 \times 0.4$  (cm) and the recording

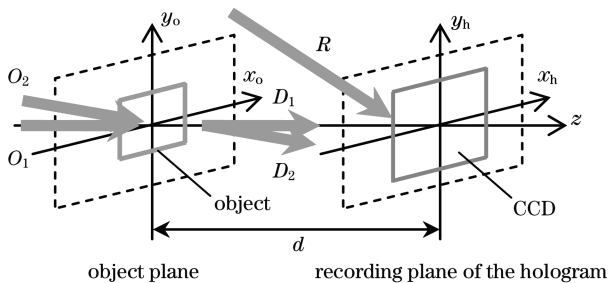


Fig. 1. Recording principle of the hologram with angular multiplexing.

distance is 90 mm. A black-white CCD with  $1626 \times 1236$  pixels and  $4 \times 4$  ( $\mu\text{m}$ ) pixel size is used to record the digital hologram. In the recording process, the object is illuminated by two plane waves in different propagation directions (one is on-axis, and the other is  $x$ -off-axis), and the angle between the two plane waves is approximately  $3.7^\circ$ .

Figures 3(a) and (b) show the recorded hologram and its spatial spectrum, respectively. The separated spectra of the two terms  $R^*D_1$  and  $R^*D_2$  corresponding to the two original object wave fields are marked by ellipses 1 and 2, respectively. After the spectrum filtering followed by an inverse Fourier transform, the reconstructed object wavefronts of the two sub-holograms in the object plane can be obtained by Eq. (3), respectively. Figures 4(a) and (b) depict the intensity distribution of the two reconstructed images, respectively. Figure 4(c) shows the reconstructed intensity image from the synthetic complex amplitudes of the two sub-holograms, and Fig. 4(d) is the regional magnified intensity image corresponding to the selected region in Fig. 4(c). It can be seen that many interfering fringes appear in Figs. 4(c) and (d), because the two reconstructed object waves have different propagation directions. So we need to use the phase correction factor  $\varphi$  mentioned above to the actual gradient angle. Figure 5 gives the final results of the complex reconstructed wave field by Eq. (6).

In our experiment, because the off-axis illumination wave is tilted along  $x$  axis corresponding to the vertical illumination wave, the change of the resolution in the horizontal direction is merely considered in the analysis of the experimental results. Figure 6(a) shows the reconstructed intensity image obtained from the sub-hologram with vertical illumination wave, and Figs. 6(b) and (c) are the partly magnified intensity images corresponding to groups 16 and 20 of Fig. 6(a), respectively. From

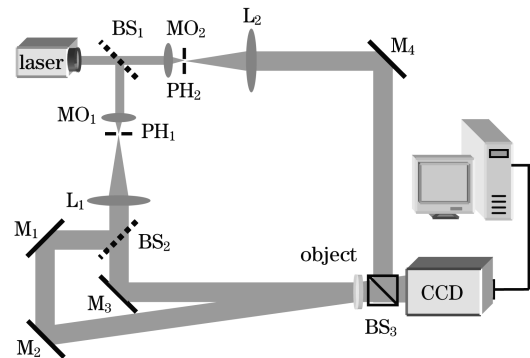


Fig. 2. Schematic of experimental setup. BS<sub>1</sub>, BS<sub>2</sub>, BS<sub>3</sub>: beam splitters; M<sub>1</sub>, M<sub>2</sub>, M<sub>3</sub>, M<sub>4</sub>: mirrors; MO<sub>1</sub>, MO<sub>2</sub>: microscope objectives; PH<sub>1</sub>, PH<sub>2</sub>: pinholes; L<sub>1</sub>, L<sub>2</sub>: lenses; CCD: camera.

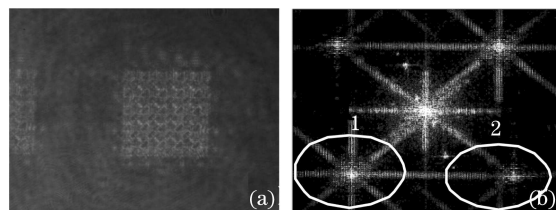


Fig. 3. (a) Recorded hologram and (b) its spatial spectrum.

Fig. 6(a), we can superlatively distinguish the upright lines of group 16, and the resolution is 59.5 lp/mm. Figure 6(d) shows the reconstructed intensity image from the synthetic complex amplitudes of the two sub-holograms via phase correction, and Figs. 6(e) and (f) are the partly magnified intensity image corresponding to groups 16 and 20 of Fig. 6(d), respectively. The upright lines of group 20 can be superlatively distinguished from Fig. 6(d), and its resolution is 74.9 lp/mm. One-dimensional (1D) intensity image along the white dashed line in Figs. 6(c) and (f) are shown in Figs. 6(g) and (h). The experimental results show that the resolution of the reconstructed synthetic image obtained with the proposed approach can be improved from 59.5 to 74.9 lp/mm in comparison with the conventional recording method with the vertical illumination wave.

According to the holographic theory, the resolution of reconstructed holographic image is significantly restricted by the target size and the spatial resolution of the CCD. Although the CCD resolution is sometimes high enough for digitally recording the interferogram, the CCD, whose target size is usually smaller than the

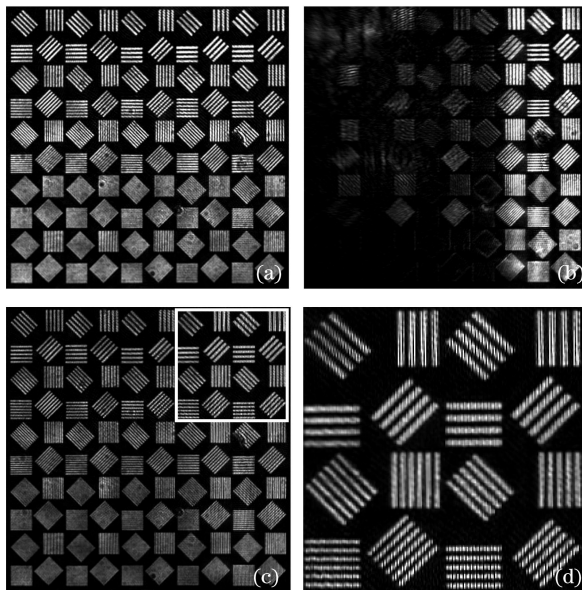


Fig. 4. Reconstructed intensity image from (a) the sub-hologram with vertical illumination wave, (b) the sub-hologram with gradient illumination wave, and (c) the synthetic complex amplitudes of two sub-holograms. (d) Regional magnification image corresponding to the selected region of (c).

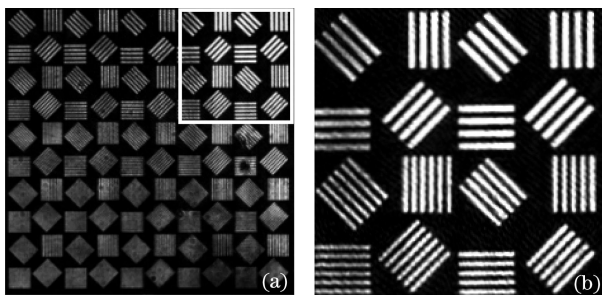


Fig. 5. (a) Intensity image of the synthetic complex amplitudes of the two sub-holograms via phase correction and (b) part corresponding magnification.

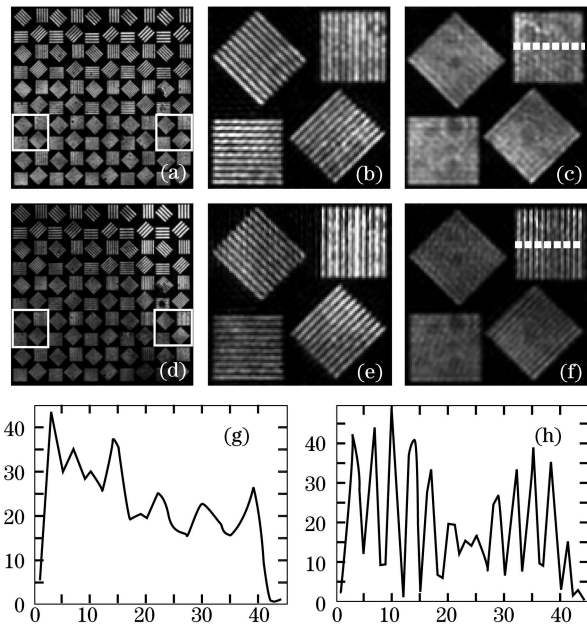


Fig. 6. (a) Reconstructed intensity image from the sub-hologram with vertical illumination wave; (b) partly magnified intensity image corresponding to group 16 of (a); (c) partly magnified intensity image corresponding to group 20 of (a); (d) intensity image of the synthetic complex amplitudes of the two sub-holograms via phase correction; (e) partly magnified intensity image corresponding to group 16 of (d); (f) partly magnified intensity image corresponding to group 20 of (d); (g) 1D intensity image along the dashed line of (c); (h) 1D intensity image along the dashed line of (f).

holographic plate, can only record part information diffracted in a certain space angle from the sample. With the proposed method, a series of sub-holograms are simultaneously recorded with multi-direction illumination on a transmitting object, and each of them covers different regions of the object spatial spectrum. This is equivalent to improving the space bandwidth product of the digital recording system and enlarging the target size of CCD, so that a higher resolution can be obtained. Furthermore, the proposed method is also applicable for the reflecting objects, and we just need to change the light illumination direction on the objects to get different range spectrum.

In conclusion, a phase correction method is presented for removing the phase slope parameter caused by the multi-direction illumination on object. The experimental results show that the phase slope occurring between the reconstructed object wavefronts of the two sub-holograms has been corrected ideally by using the proposed method, and the resolution of the reconstructed synthetic image has been improved obviously.

This work was supported by the Science Foundation of Aeronautics of China under Grant No. 2006ZD53042.

## References

1. J. W. Goodman and R. W. Lawrence, *Appl. Phys. Lett.* **11**, 77 (1967).
2. U. Schnars and W. Jüptner, *Appl. Opt.* **33**, 179 (1994).
3. T.-C. Poon, *Digital Holography and Three-Dimensional Display* (Springer, New York, 2006).

4. J. Di, J. Zhao, Q. Fan, H. Jiang, and W. Sun, *Acta Opt. Sin.* (in Chinese) **28**, 56 (2008).
5. T.-C. Poon, K. B. Doh, B. W. Schilling, M. H. Wu, K. Shinoda, and Y. Suzuki, *Opt. Eng.* **34**, 1338 (1995).
6. B. W. Schilling, T.-C. Poon, G. Indebetouw, B. Storrie, K. Shinoda, Y. Suzuki, and M. H. Wu, *Opt. Lett.* **22**, 1506 (1997).
7. T. Zhang and I. Yamaguchi, *Opt. Lett.* **23**, 1221 (1998).
8. C. Qin, J. Zhao, J. Di, L. Wang, Y. Yu, and W. Yuan, *Appl. Opt.* **48**, 919 (2009).
9. J. Zhao, H. Jiang, and J. Di, *Opt. Express* **16**, 2514 (2008).
10. Z. Li, F. Xia, G. Zheng, and J. Zhang, *Chin. Opt. Lett.* **6**, 251 (2008).
11. F. Joud, F. Laloë, M. Atlan, J. Hare, and M. Gross, *Opt. Express* **17**, 2774 (2009).
12. F. Le Clerc, M. Gross, and L. Collot, *Opt. Lett.* **26**, 1550 (2001).
13. L. Zhong, Y. Zhang, and X. Lü, *Chinese J. Lasers* (in Chinese) **31**, 1207 (2004).
14. C. Yuan, H. Zhai, and H. Liu, *Opt. Lett.* **33**, 2356 (2008).
15. V. Mico, Z. Zalevsky, P. Garcia-Marinez, and J. Garcia, *Opt. Express* **12**, 2589 (2004).
16. C. Liu, Z. Liu, F. Bo, Y. Wang, and J. Zhu, *Appl. Phys. Lett.* **81**, 3143 (2002).